

Modelling methods for determining fault management requirements in future MEA and MEE platforms

M. Szykiel (1), S. D. A. Fletcher (1), P. J. Norman (1), S. J. Galloway (1), G. M. Burt (1)

1: University of Strathclyde, 99 George Street, Glasgow, Scotland, G1 1RD, michal.szykiel@strath.ac.uk

Abstract This paper presents a modular transient modelling tool which provides model-based support for the design and technology selection within future MEE and MEA electrical systems. The developed tool is a Matlab/Simulink library consisting of functional sub-system units, which can be rapidly integrated to build complex system architecture models. The paper focusses on the ability of the tool to assess the thermally-defined fault withstand capability of power electronic converters in order to inform on technology trades and derive the operating requirements of the associated power system protection/fault management devices.

Introduction

As the More-Electric Aircraft (MEA) and More-Electric Engine (MEE) concepts progress [1], the electrical architectures on the next generation of aircraft will undergo significant changes.

These design changes are partly driven by emerging enabling technologies, such as novel electrical machines, power dense power electronic converters and solid state circuit breakers. Whilst these technologies may offer advantages, the broad range of different technology solutions available also causes the design of these electrical systems to become increasingly complex. Consequently, a large number of studies can be required to properly identify an optimal set of devices within the variety of possible system configurations [2].

The integration of new technologies into a system design also introduces a potential range of new failure cases and with significantly different electrical fault behaviour. The understanding of these fault cases and development of appropriate methods to manage these faults is also a significant challenge for the future aircraft electrical systems.

This paper presents a modular transient modelling tool (MTM) which is designed to support this complex design process. The tool allows rapid modelling of MEE and MEA power systems using modular blocks. This enables the rapid evaluation of many design options over a range of test scenarios.

The paper then demonstrates how the MTM tool can be used to assess the fault tolerance, and subsequent protection requirements, of different ac/dc rectifier design options within an example aircraft electrical network.

Overview of the Modular Transient Modelling (MTM) Tool

Within the MTM tool, different electrical subsystems

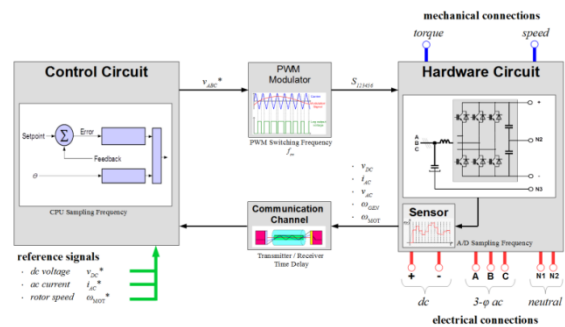


Fig. 1: MTM tool subsystems design structure

are modelled using a common internal structure. This is illustrated in Figure 1. Within this structure each subsystem consists of five types of modules:

- *Hardware Circuit* - electrical circuit of sub-systems modelled with SimPowerSystems toolbox [3]. It is used to represent electrical circuitry of the subsystem components, i.e. power electronics converter, machine drives.
- *Sensor* - measures controlled instantaneous signals along with the errors caused by A/D sampling, signal saturation, etc.
- *Communication* – signal transmission between sensor and control circuit, which may include modelling delays and communication errors.
- *Control Circuit* – the algorithm used to control the operation of machine exciter or power electronics. Each subsystem has individual control command.
- *Modulator* – used to convert the reference signal into logic binary signals associated to each single switch.

Splitting up the electrical subsystem models in this way allows individual modules to be easily changed without impacting the design of other aspects of the subsystem. This enables the influence of different designs to be quickly tested and understood.

Dynamic Electro-Thermal Modelling

As well as providing detailed electrical transient modelling capability, the MTM tool allows the thermal behaviour of the electrical components to be modelled. This enables the impact of adverse network conditions on the components, such as electrical faults, to be quantified and the required fault withstand to be better understood.

By way of an example, this section describes how this is achieved for power converters using dynamic junction temperature and power loss estimation models. These models have been developed to measure and record the transient junction temperature and the variations in power loss of each individual semiconductor during normal and fault conditions.

The electro-thermal model calculates the transient temperature change based on estimated instantaneous power losses, from the instantaneous output current $i(t)$, voltage $v(t)$, temperature $T_j(t)$, and other parameters, such as component thermal resistance, which can be found in manufacturers' datasheets.

Figure 2 illustrates the outline structure of the developed device electro-thermal model. This proposed power loss modelling approach is consistent with that presented in [4,5], which is a commonly accepted method for loss evaluation of power semiconductor devices.

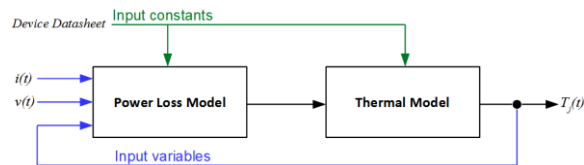


Fig. 2: Top-level flow chart used to estimate power losses and junction temperatures

The dissipated energy values are determined using three-dimensional look-up tables which have been developed using the device characterisation data in manufacturer datasheets. The loss models of the diodes are designed in a similar way. Note that these models are not designed to capture forward recovery losses generated during the turn-on as these are considered negligible and normally neglected for switching frequencies below 400 kHz [6].

During normal operation, the electro-thermal model can be used to estimate power losses and junction temperature levels. During abnormal operation, the thermal model of a single device is capable of

indicating the rate of rise of junction temperature, for example when the device is subjected to excessive fault current. Figure 3 illustrates the developed model. The thermal impedance from junction to ambient $Z_{th(j-c)}(t)$ is modelled as a six-layer Foster RC network [4,5]. The Foster network is a partial fraction circuit consisting of series-connected RC elements. Such a network allows accurate estimation of the temperature rise between these points.

The thermal resistance R_{th} will determine the steady state value of junction temperature and the thermal time constant τ_{RC} . The τ_{RC} can be calculated from

$$\tau_{RC} = R_{th} \cdot c_{th} \quad (1)$$

This will dictate the dynamic change of the junction temperature T_j .

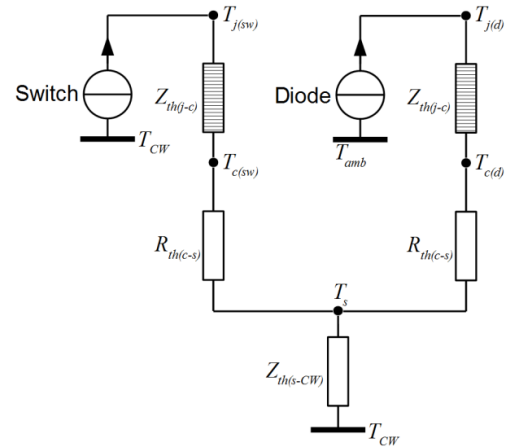


Fig. 3: Thermal circuit model for the semiconductor power modules.

The inlet coolant temperature, T_{CW} , is assumed constant for both steady state and fault conditions, due to the fault's relatively short duration. The RC parameter values of semiconductor junction-case transient thermal impedance $Z_{th(j-c)}(t)$ can be found directly from the manufacturers' datasheets [7-10].

The thermal resistance value of the selected cooling systems cold plate $R_{th(s-CW)}$ can also be obtained directly from manufacturers' datasheets. The models used in the subsequent sections will utilise the tube liquid cold plate described in [11] as an example.

The thermal capacitance of the component cooling system can be approximated from

$$C_{th(s-CW)} = m_s \cdot c_s \quad (2)$$

where m_s is mass and c_s is the specific heat of the selected cold plate material. The transient junction temperature rate of change $\Delta T_j(t)$ is estimated from

$$\Delta T_j(t) = P_d(t) \cdot \sum_{i=1}^6 R_{th(i)} \cdot \left(1 - e^{-t/R_{th(i)} \cdot C_{th(i)}}\right) \quad (3)$$

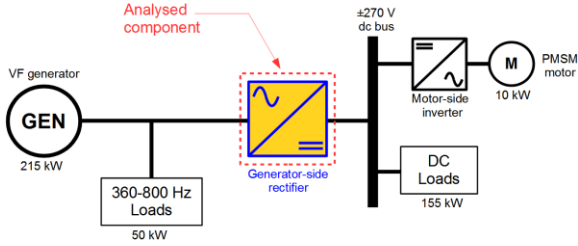


Fig. 4: Example network representation of the modelled MEE/MEA power system

with the total dissipated power $P_d(t)$ made by switching and conduction losses.

Junction Temperature Variations during Faults

The developed MTM dynamic electro-thermal model for solid state devices can be both used for the sizing of the converter components and the characterisation of device dynamic thermal behaviour under fault conditions. This second feature will be illustrated further in this section. For this purpose the example electrical network shown in figure 4 will be utilised, with the simulation results focusing on the response of the main power converter supplying the ± 270 VDC bus.

Within this network, the capability provided by the MTM tool enables:

- Evaluation of fault tolerant operation
- Specifications of parameter settings for overload and fault protection systems.
- Identification of timing sequence for fault management optimal response.
- Specifications of power electronics cooling system design

Figure 5 illustrates the effect of a simulated 1-phase short circuit ac fault on the analysed rectifier and dc network.

The fault causes the ac line voltage on the affected phase to collapse. This also results in a voltage drop across the dc distribution bus. Subsequently, the rectifier *Control Circuit* module commands a higher current to flow through the switches in healthy phases in order to maintain constant dc voltage across the ± 270 VDC distribution system.

The increased currents flowing through the semiconductor switches result in a rise in their

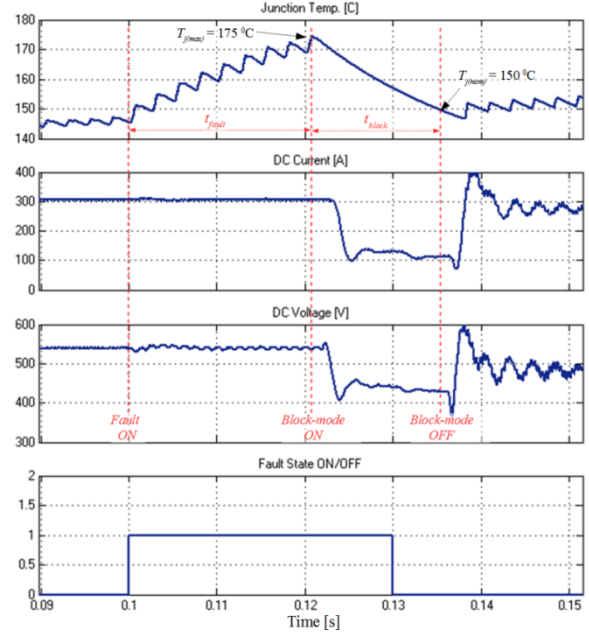


Fig. 5: Post-fault behaviour during ac fault on the generator-side rectifier with INFINEON FL300R [7].

junction temperature. If the fault is not cleared quickly enough by the network protection system, the junction temperature may exceed the maximum limits of $T_j(t) > 175^\circ\text{C}$ and lead to the activation of the converter block-mode. This would cause all semiconductor switches to be turned off and the converter to be temporarily out of service [12]. Until the junction temperature of the solid state switches drops down to a safe level ($T_j(t) < 150^\circ\text{C}$), the rectifier cannot provide the required amount of power to the dc distribution system.

Table 1 presents the measured periods, from fault inception until the junction temperature rises above 175°C , t_{fault} , and the duration of the rectifier's fault recovery period, t_{block} , for each analysed set of solid state switches. During the fault recovery period, the rectifier is out of service and ancillary power must be used to supply the electric loads. The results can be used to support the design of fault protection schemes, optimise fault management system or determine cooling system and inductor size requirements for fault tolerant operation.

Table 1: Simulation results of different ac/dc rectifier variants for optimal fault management system design

Device	Min. fault-tolerant period t_{fault} [ms]	Max. fault-recovery period t_{block} [ms]
INFINEON FL300R [7]	21.1	15.21
SEMIKRON SKM301ML [8]	18.7	24.34
ROHM BSM300D [9]	0.363	2.203
CREE CAS300M [10]	0.401	6.129

The results also show that analysed SiC devices tend to both heat up and cool down much faster than the presently utilized Si-based semiconductors. This is due to the inherent short transient thermal time constants t_{RC} of the SiC MOSFETs in conjunction with high switching frequency $f_{sw} = 38$ kHz and results in its rapid overheating within the first millisecond of fault occurrence. For this condition to be avoided, a fast-acting protection unit would be required.

For the scenario where the ac/dc rectifiers are equipped with Si IGBTs, the longer transient thermal time constant allows the rectifier to continuously operate and supply the power 15 ms after the fault occurrence.

The maximum registered fault recovery period of SiC devices is approximately 6 ms. After being shut down, the rectifier is able to recover three times faster than the rectifier containing Si devices. This demonstrates that the rectifier built from Si devices has higher fault tolerant capability, while the equivalent rectifier made of conventional SiC devices has higher capability for fault recovery. The priority and importance of each feature needs to be examined in detail against individual requirements of the selected electrical loads in MEE/MEA power system in order to optimise fault management strategy.

Summary

This paper has presented an approach for simple and fast transient modelling of complex MEA and MEE architectures for simulation-based studies. The modelling strategy relies on splitting the system into functional sub-systems, enabling a wide range of technologies and control techniques to be readily tested. The electro-thermal modelling aspect of the MTM tool also allows comprehensive fault studies to be conducted to clearly demonstrate the impact of faults on individual components in a given electrical network design. The paper highlights one application of this tool through the comparison of the fault tolerance of different ac/dc rectifier designs. The generated results can be used to trade off the requirement for individual converter fault tolerance against the network's wider fault management requirements including fault isolation and re-connection back-up power supplies.

Acknowledgement

This work has been carried out as part of the Rolls-Royce UTC program.

References

1. B. Bhangu, K. Rajashekara, "Electric Starter Generators: Their Integration into Gas Turbine Engines," IEEE Ind. App. Mag. 20(2): 14-22, 2014.
2. I. Moir, A. Seabridge, "Aircraft Systems: Mechanical, Electrical and Avionics Subsystems Integration," (Aerospace Series, Wiley, 2008), pp. 182, ISBN: 0470770945.
3. Mathworks Inc., MATLAB (Version R2014a), Computer Software, 2014. www.mathworks.com
4. A. Stupar, D. Bortis, U. Drogenik, J. Kolar, "Advanced setup for thermal cycling of power modules following definable junction temperature profiles," IPEC 2010, June 21-24, 2010.
5. S. Yin, T. Wang, K. Tseng, J. Zhao, et al., "Electro-thermal modeling of SiC power devices for circuit simulation," IECON 2013, November 10-13, 2013.
6. J. Jordan, J. Magraner, C. Cases, V. Esteve, et al. "Turn on switching losses analysis for Si and SiC diodes in induction heating inverters," EPE 2009, Spain, September 8-10, 2009.
7. INFINEON F3L300R07PE4 datasheet, available at: <http://infineon.com/>, accessed Mar. 2016.
8. SEMIKRON SkiM301MLI07E4 datasheet, available at: <http://semikron.com/>, accessed Mar. 2016.
9. ROHM BSM300D12P2E001 datasheet, available at: <http://rohm.com/>, accessed Mar. 2016.
10. CREE CAS300M12BM2 datasheet, available at: <http://cree.com/>, accessed Mar. 2016.
11. Aavid Thermalloy, "Tube Liquid Cooling 418101U00000G" datasheet, available at: <http://aavid.com/>, accessed Mar. 2016.
12. K. Wang, Y. Liao, G. Song, X. Ma, "Over-Temperature protection for IGBT modules," PCIM 2014, May 20-22, 2014.